Coupling of the magnetic field and gas flows inferred from the net circular polarization in a sunspot penumbra

Shaltout, A. M. K.; Ichimoto, K.

COUPLING OF THE MAGNETIC FIELD AND GAS FLOWS INFERRED FROM THE NET CIRCULAR POLARIZATION IN SUNSPOT PENUMBRA

A.M.K. Shaltout[1,2*] and Kiyoshi Ichimoto[1]

[1]Kwasan and Hida Observatories, Kyoto University, Kurabashira Kamitakara-cho, Takayama-city, 506-1314 Gifu, Japan.

[2]Department of Astronomy and Meteorology, Faculty of Science, Al-Azhar University, Nasr City, Cairo, Egypt, 11884.

ABSTRACT

We analyze the penumbral fine structure using high resolution spectropolarimetric data obtained by the Solar Optical Telescope aboard Hinode. The spatial correlation between the net circular polarization (NCP) and Evershed flow channels are investigated in detail. **Here we obtain that a negative NCP structures are correlated with the Evershed flow channels in the limb-side penumbra and a negative NCP or depression of positive NCP is associated with the Evershed flow channels in the disk center-side of the penumbra for a negative-polarity sunspot in NOAA 10923.** The positive NCP structures in the disk center-side penumbra are essentially attributed to interflow channels instead of Evershed flow channels. ~~**However,**~~ **our result is not consistent with the ~~embedded flux tube model of~~ penumbra in which the penumbral NCP is created ~~entirely~~ in the Evershed flow channels.** The stratifications of magnetic field and velocity are investigated by using SIR-JUMP inversion with one-component atmospheres, and thus to reproduce the NCP of spectral lines in the limb-side and disk center-side of the penumbra. The inversion results show that the increased Evershed flow is associated with a stronger magnetic field located preferentially in the deep photosphere. Our result is controversial to the simple two component penumbral models in which the Evershed flow essentially creates the global NCP in sunspots.

Subject headings: Sun: sunspots – line: profiles - Sun: magnetic fields – Sun: visible

*Email: shaltout123@gmail.com

1. Introduction

High resolution observations of sunspot penumbra revealed that the Evershed flow, a conspicuous horizontal outflow in the deep photospheric layer, is clearly related to the penumbral filaments (Title et al. 1992; Shine et al. 1994; Tritscher et al. 2004; Langhans et al. 2005; Rimmele and Marino 2006; Ichimoto et al. 2007a). Magnetic and flow fields in penumbra have been studied to understand the origin of the filamentary structure of penumbra and of the Evershed flow observed at the photospheric layers (see for the review, Solanki 2003; Borrero and Ichimoto 2011), and the recent high resolution observations by Hinode and ground based telescopes revealed that the Evershed effect and the penumbral filamentary structure could be understood as a natural consequence of thermal convection under a strong, inclined magnetic fields in sunspot (Ichimoto et al. 2007b; Borrero et al. 2008; Scharmer et al. 2008; Rempel et al. 2009; Ichimoto 2010; Spruit et al. 2010).

The properties of penumbral filaments were determined indirectly from spectropolarimetric measurements as regards of the two-component model atmospheres under a relatively poor spatial resolution achieved by ground-based instruments (see e.g., Bellot Rubio et al. 2004, 2006; Borrero et al. 2004, 2006; Beck 2011). Jurcak et al. (2007) and Borrero et al. (2008) have studied for the first time the penumbral fine structure by means of the one-component model atmospheres using data obtained by the Solar Optical Telescope (SOT; Tsuneta et al. 2007) on board Hinode. Those works found a weaker and horizontal magnetic field along with an increased line of sight (LOS) velocity, i.e., the Evershed flow that is driven by the convectively rising hot gas is weakly magnetized. In contrast, Borrero and Solanki (2008) found

an increasing magnetic field strength along with the optical depth near the continuum level in Evershed flow channels using observations taken by SOT (see, for the recent review, Solanki 2003; Borrero and Ichimoto 2011).

The net circular polarization (NCP), a measure of the asymmetry of the Stokes V polarization signal, is an important source of information on the three-dimensional organization of the solar magnetic field structures. The NCP is generated by gradients with optical depth in the line-of-sight (LOS) velocity and magnetic field vector and it sign also depends of the sign of those gradients (e.g., Auer and Heasley 1978; Skumanich and Lites 1987; Sanchez Almeida and Lites 1992). Spectropolarimetric observations of sunspot penumbra clearly show one of the largest NCP values of all solar structures (Illing et al. 1974; Auer and Heasley 1978; Henson and Kemp 1984; Sanchez Almeida and Lites 1992). Early observations of the sunspot NCP from the ground show that the largest NCP occurs in the limb-side penumbra with the same sign as the umbra's blue lobe of the Stokes V profile while the disk center-side penumbra shows opposite sign of NCP to that of the limb-side penumbra (Martinez Pillet 2000). The most successful explanation is found in models where the magnetic field inclination changes along the depth together with the LOS velocity, i.e., the Evershed flow is concentrated in deep layers in embedded flux tubes, in which the magnetic field is nearly horizontal and its strength is weaker or nearly the same with the overlaying layer (Solanki and Montavon 1993; Martinez Pillet 2000; Müller et al. 2002; Müller et al. 2006). The opposite sign of NCP between limb-side and disk center-side penumbra is attributed to the opposite sign of LOS velocity of the Evershed flow in these models.

High resolution observation of the NCP in a penumbra is reported by Tritschler et al. (2007), Borrero et al. (2007) and Ichimoto et al. (2008). They concluded that the filamentary

structure of the penumbra is clearly noticeable in both LOS velocity and NCP images. Ichimoto et al. (2008) showed from Hinode data that the flow channels in both center-side and limb-side penumbra are correlated with the same sign of NCP, and opposite sign of NCP in center-side penumbra is spatially attributed to interflow channels (spines). This result evidently contradicts with what the embedded-flux-tube model predicts. Tritschler et al. (2007) also found the fine scale fluctuations in the NCP and Doppler signals, but they do not find a significant spatial correlation between the NCP and LOS velocity due to insufficient spatial resolution data, as explained in their paper.

Another penumbral model controversial with the embedded flux-tube model is the field-free gap model (e.g. Scharmer & Spruit 2006; Spruit et al. 2010), which has been proposed to explain the penumbral fine structure. Scharmer & Spruit (2006) and Spruit & Scharmer (2006) suggested that the penumbral bright filaments are modeled as field-free gaps that appear below the penumbral magnetic field, but no indication was shown that this model finally reproduces the observed NCP. Moreover, as already pointed out in Borrero & Solanki (2008), this model predicts a weaker magnetic field strength with optical depth in the line-forming region because the magnetic field inside the gap is always very close to zero.

In a numerical simulation, the filamentary structure of penumbra that harbor the Evershed flows reveals a nearly horizontal plasma outflow of several km s^{-1} which is associated with a more inclined field (Rempel et al. 2009). The numerical 3-D MHD simulations exhibit a stronger and more horizontal magnetic fields associated with increased LOS velocities at optical depth unity (see, Rempel 2011, for further details).

In this paper, we investigate the NCP of a sunspot in Fe I lines at 6302 Å using a data set of spectropolarimetric observations by SOT in a sunspot penumbra at heliocentric position of S 7.5^{o}

and W 16.1°. We focus on the spatial correlation between the NCP and Evershed flow to settle the validity of the current understanding of the relation between NCP and the penumbral fine structures. Stratifications of physical quantities that reproduced the observed NCP are investigated for Evershed flow and interflow channels by applying Stokes inversion code, SIR-JUMP, to the observed Stokes profiles. The observations are described in Section 2. The spatial correlation between the NCP and Evershed flow is discussed in Section 3. The Stokes inversion and the results of the fitting are explained in Section 4. Finally, summary and conclusion are presented in Section 5.

2. Observations

A negative-polarity sunspot in the active region NOAA 10923 was observed on Nov. 15, 2006 with the spectropolarimeter (SP) of the Solar Optical Telescope (SOT; Tsuneta et al. 2007; Suematsu et al. 2007) aboard Hinode (Kosugi et al. 2007). The SP recorded full Stokes profiles of the pair of Fe I lines at 630.15 nm (effective Landé factor g = 1.67) and 630.25 nm (g = 2.5) with a photometric accuracy of ~ 0.1 % and a spatial sampling of 0.16 arcsec/pixel. The sunspot was located at heliocentric angle of around 17.9° away from the disk center at the time of the observation.

The spectral resolution is 22.13 mÅ/pixel. The field of view (FOV) of the SP observation is 110" x 164" with a slit oriented in North-South on the heliographic disk. The integration time at each slit position is 4.8 s (normal mode). It took about 60 minutes with 689 slit steps to map the FOV. The SP data are calibrated with the standard routine, SP_PREP (Lites and Ichimoto 2013), available under the Solar Software (SSW).

3. The correlation analysis between Evershed flow and NCP

The NCP, a measure of the asymmetry of the Stokes-V line profiles, is defined by NCP

$=\int(\frac{V}{I_c})d\lambda$, where I_c is the continuum intensity and the integral include only the Fe I line at 630.25 nm in this study. The LOS velocity image was obtained from the bisector position of the line wing at the intensity level of 0.8 times line-depth from the line core of 630.15 nm, where we take the position of the center of gravity of this line averaged over the quiet Sun and shifting it by -200 m s^{-1} to get a reference position of the spectral line. This value corresponds to the gravitational red-shift plus the convective blue-shift of the line (Borrero et al. 2004). We focus on the spatial correlation between the NCP and Evershed flow as was done by Ichimoto et al. (2008) but in more comprehensive manner by employing a correlation analysis. Fig. 1 shows continuum intensity, Doppler shift and NCP maps of the sunspot. Filamentary structures are obvious in the continuum intensity, LOS velocity and NCP in the penumbra. It is evident in the Dopplergram that the limb-side penumbra is dominated by radially elongated penumbral filaments with positive LOS velocity. In contrast, the disk center-side penumbra reveals elongated penumbral filaments with negative LOS velocity in the radial direction of the sunspot. Penumbral filaments exhibit the strongest evidence of the negative NCP in the limb-side penumbra, while the disk center-side penumbra is moderately enhanced by positive NCP, but negative NCP structures are also present. Blue and red contours in the bottom - right panel of Fig. 1 identify regions with -1.5 (blue) and 0.8 km s^{-1} (red) LOS velocities. When comparing the NCP maps with the overlaid contours of LOS velocity, it is noticed that the limb-side penumbra shows negative NCPs associated with the Evershed flow channels (redshifted velocities). While the Evershed flow channels (blueshifted velocities) in the disk center-side penumbra tend to be correlated with the negative or smaller positive NCP structures again.

Given advantage of the high resolution observations, it is interesting to perform a study of the correlation coefficient (CC) between the NCP and LOS velocity associated with the

penumbral fine structures. Correlations are computed using the full resolution of Hinode data inside a small box, which has 10 pixels width and height, and the procedure was taken over the penumbra and therefore to present a CC map for the penumbra. The reason for selecting 10 x 10 boxes is to include a large number (100) of pixels inside this box for a better definition of the correlations. The right panel of Fig. 2 shows CC map thus obtained; penumbral filaments show a negative correlation in the limb-side penumbra, owing to a positive LOS velocity being found in regions with a negative NCP. The disk center-side penumbra mostly exhibits a positive correlation; especially the robust evidence of the positive correlation is seen in the middle part of the disk center-side penumbra. The specific reason for this is that a negative LOS velocity (=Evershed flow) is correlated with a negative NCP in the middle part of the penumbra in high spatial resolution, and then overall CC is positive there. Also noticed are a number of small patches of negative correlations near the inner edge of the disk center-side penumbra, while similar results in a reduction of the correlation (i.e., negative sign) are found at the outer edge of the penumbra. Our present result is consistent with that of Ichimoto et al. (2008) though they reported no indication of a sign change along the radial distance in the penumbra. The main source of the positive NCP found in the disk center-side penumbra is thus attributed to the interflow channels instead of the Evershed flow. This constitutes for the presence of gas flows in the interflow channels in the penumbra. Observations used here contain a negative-polarity sunspot observed by Hinode, hence the opposite polarity sunspot changes signs of NCP in the penumbra.

Here we present in Fig. 3 the distributions of azimuthally averaged NCP and CC along the radial distance from the center of the sunspot for both of disk center-side (solid lines) and limb-side (dashed lines) of the penumbra. The region used for the azimuthal mean is shown in

the Doppler image in Fig. 2. A radial distance of zero arcsec indicates the inner boundary of the penumbra, while the radial distance of 18 arcsec indicates the outer boundary of the penumbra. We also plot a curve for the flow-channels (curve with triangle) and another for the interflow channels (curve with diamond) for the NCP, where the Evershed flow and interflow channels are identified by local maximum and local minimum of the Doppler shift in the limb-side, and by local minimum and local maximum in the disk center-side penumbra, respectively. The criteria for selecting the local minimum and maximum is ± 0.01 km/sec/pixel^2 in the second derivative of the Doppler shift along each arc, respectively.

Left panel of Fig. 3 exhibits the azimuthally averaged NCP in the disk center-side (solid line) and limb-side penumbra (dashed line). In the limb-side penumbra, for both Evershed and interflow channels, the NCP shows a sharp increase in negative sign in the inner penumbra and eventually decreases slowly with radial distance towards the outer edge, while it is evident that the Evershed flow channels have larger negative NCP than interflow channels throughout the penumbra. The NCP in the disk center-side penumbra, for the Evershed and interflow channels together, shows a gradual reduction of positive NCP with radial distance at the inner part of penumbra and then it changes sign to get a negative NCP towards the outer edge of penumbra. The solid line marked with triangles clearly shows that the NCP for the Evershed flow channels display a decrease of positive NCP in the middle part of penumbra as compared with the interflow channels (solid line marked with diamonds).

Finally, the right panel of Fig. 3 shows the azimuthally averaged correlation coefficients (CC) obtained from the CC map of Fig. 2, right panel. We notice large fluctuations of the CC value along each arc in both sides of penumbra. The limb-side of the penumbra (dashed line) clearly displays negative CC with its peak of CC = -0.6 around 3-10 arcsec while it reaches -0.1

at the outer edge of penumbra. The disk center-side penumbra (solid line) is dominated by a positive CC with the value of about 0.1-0.4, though it exhibits a negative value at the innermost part.

4. Fitting of Stokes profiles with synthetic models

The observed Stokes profiles of Fe I lines at 630.15 and 630.25 nm were fit using the SIR-JUMP, which is a modified version of SIR (Stokes Inversion based on Response functions; Ruiz Cobo & del Toro Iniesta 1992). Under the assumption of local thermodynamic equilibrium (LTE), SIR-JUMP employs a Levenberg-Marquart nonlinear least-squares (merit function, χ^2) minimization algorithm (Press et al. 1986), where the partial derivatives of the Stokes parameters with respect to the various atmospheric parameters are calculated through analytic response functions (see Ruiz Cobo & del Toro Iniesta 1992). The inversion code iteratively modifies an initial guess model atmosphere by means of response functions until the synthetic spectrum matches the observed one. To explain the observed NCP, the inversion code assumes the existence of jumping perturbation (JP) in the stratifications of physical parameters in the line forming region. We only consider one magnetic field component in each pixel inside the penumbra (called “one-component atmospheres” in the following) since it could be a good assumption for the high resolution measurements taken by Hinode satellite. This assumption has been used to study the structure of sunspots penumbra by using the Hinode measurements (see, Jurcak et al. 2007; Borrero et al. 2008; Borrero & Solanki 2008).

The initial guess temperature model is taken from the mean penumbral model derived by del Toro Iniesta et al. (1994). The total number of free parameters that the inversion retrieved from the observed Stokes profiles is 14, while the influence of the height independent

macroturbulent velocity and stray-light factor are neglected in this analysis. The physical parameters that define the initial atmosphere are constant with optical depth in the line-forming region (field strength B, inclination γ, azimuth ϕ and LOS velocity v_{LOS}), where we took these values from the Milne Eddington inversion results. We adopt only four nodes for the perturbation of the temperature stratification in the inversion code. The perturbation is identified by the amplitude and position of the jump in the physical quantities across the optical depth. In addition to the free parameters mentioned above, the position of the discontinuity is a free parameter. The amplitudes of jump provide five free parameters, where we adopt the following amplitudes of JP in the stratification of the physical parameters: (ΔB, $\Delta\gamma$, $\Delta\phi$, Δv_{LOS}, v_{mic}). We have inverted 264 pixels covering two azimuthal cuts in the limb-side and disk center-side at the middle part of the penumbra (Fig. 2). The reason for this is that a significant feature is seen at the middle disk center-side and limb-side penumbra, where CC map (Fig. 2, right panel) shows negative and positive CC values and it is also possible to sample many Evershed flow channels and interflow channels at the same radial distance.

In Figs. 4 and 5, we show the observed Stokes *I*, *Q*, *U* and *V* profiles (circles) and synthetic profiles produced by SIR-JUMP (solid lines) for the 2 points representing the Evershed flow and interflow channels in the limb-side penumbra, respectively. The three components of the vector magnetic field (strength, inclination, and azimuth) together with the LOS velocity derived from the inversion are presented as a function of the optical depth in Figs. 6 for both the Evershed flow and interflow channels in the limb-side penumbra, where the physical parameters of the Evershed flow channels are shown by solid lines and those of the interflow channels by dashed lines. The inclination of the field was defined with respect to the line-of-sight (LOS), where zero degree means a magnetic field towards us and 180 deg. means a magnetic field away from us.

The NCPs are evaluated from the observed and synthetic Stokes-V profiles and are presented in the top right panels of Figs. 4 and 5. Fairly good agreements of the NCPs obtained from the observed and synthetic Stokes-V profiles ensure that the one component model is well reproduced the observed Stokes profiles for the positions selected in the limb-side penumbra.

As can be realized in Fig. 6, the LOS velocity shows the presence of strong, confined Evershed flows in the deep layer of the photosphere with velocities of up to 3 km s^{-1}. Interestingly, the strong flows take place with the existence of strong magnetic field around 2000 G. Fig. 6 displays the inclination discontinuity is about 31 deg. The azimuth of the magnetic field is found to be almost constant along the LOS. In the interflow channel in the limb-side penumbra, the flow in deep layer is about 1 km s^{-1}. The inclination discontinuity is small (about 15 deg.) in the interflow channels. Our analysis shows that the deep part of the interflow channel has weaker magnetic field strength than the Evershed flow, and smaller jump of the field strength.

Similarly, here we analyze the Evershed flow channels in the disk center-side penumbra. The fitting results in Evershed flow channel are given in Fig. 7, where Stokes profiles calculated from two different solutions are shown with solid and thick dashed lines. The stratifications of the physical parameters of the atmosphere for the two solutions are displayed by solid and dashed lines in Fig. 8. Solid line in Fig. 8 displays the stratifications of one such solution exhibiting large blueshifted velocities exceeding -2 km s^{-1} in the deeper layer that is associated with a weaker magnetic field of 1700 G. While the other solution (dashed lines) reveals LOS velocities of -1.4 km s^{-1} associated with a strong magnetic field around 2200 G in deep layer. In the top right panel of Fig. 7, displayed are two calculated NCP values (0.16 mÅ for solid lines and 0.97 mÅ for thick dashed lines) compared with the observed one. In fact, the fitting results

of the Stokes profiles (solid and thick dashed lines) are very close to each other and almost indiscernible.

Finally, it is adequate to display here the Stokes profiles and physical parameters of the fitting result for an interflow channel in disk center-side penumbra, since the positive NCP is attributed to this region. The Stokes profiles and fitting results are shown in Fig. 9, while the magnetic field configurations inferred from the interflow channels in the disk center-side penumbra are presented by solid lines in Fig. 10. The one-component atmosphere gives a reasonable fitting of the Stokes-V profiles and a successful matching between the observed and synthetic NCP. It is noticeable that the interflow channels in the disk center-side penumbra have a large blueshifted flow in deep layer associated with a weak magnetic field and such stratification is responsible for the positive NCP.

To clarify how well the inversion consequences reproduce the observed NCP, we plot in the left panel of Fig. 11 the calculated NCP from the inversion result against the observed values for all pixels along the two azimuthal cuts shown in right panel of Fig. 2. Data in the limb-side and disk center-side penumbra are shown by asterisks and diamonds, respectively. It is noticeable that the calculated NCP is fairly well correlated with the observed one for the limb-side penumbra, while for the disk center-side penumbra the reproduced NCP is noticeably smaller than the observed NCP. Beck (2011) also noticed that a better reproduction of the NCP is found in the limb-side penumbra, while the disk center-side is less well reproduced.

Correlation between the observed NCP and the LOS velocity is shown in the middle panel of Fig. 11. A positive correlation in the disk center-side and a negative correlation in the limb-side penumbra are evident confirming the result of CC map in Fig. 2. Right panel of Fig. 11 shows the amplitude of discontinuity of the field strength (dB = B (deep layer) - B (upper layer))

against the LOS velocity in the limb-side (asterisks) and disk center-side (diamonds) penumbra. It is clear in the limb-side penumbra that large LOS velocities (Evershed flow) have a positive dB. In contrast, in the disk center-side penumbra, the correlation between dB and LOS velocity is rather poor while most pixels have a positive dB. Referring to the fact that the inversion result in the limb-side shows essentially more robust and consistent results in which the flow channels are associated with a strong magnetic field in deep penumbra, while it is difficult to conclude a robust result due to the ambiguity (= non uniqueness of solution) of inversion, as displayed in Fig. 7 in disk center-side penumbra, and since there must be no intrinsic difference in physical condition between limb-side and disk center-side penumbra, we interpret that the solution in the disk center-side may not represent the real structure of the penumbra.

5. Discussion and Conclusion

Taking the advantage of the high spatial resolution of Hinode SP, we examined the spatial correlation between the NCP and Evershed flow (=LOS velocity) for a penumbra of a negative-polarity sunspot located at a heliocentric angle of 17.9 deg. **From a cross-correlation analysis, we demonstrate that the Evershed flow channels create a negative NCP in the limb-side and ~~a negative or less positive NCP~~ in the disk center-side penumbra.**

We have determined the physical parameters of a sunspot penumbra from the inversion of Stokes profiles. In order to keep the number of free parameters at minimum, SIR-JUMP with one-component atmospheres is used for this purpose. The inversion results for the Evershed flow channels show that the deep layers in the limb-side penumbra has LOS velocities exceeding 3 km s^{-1}, while in the disk center-side penumbra this component reveals velocities close to -2.5 km s^{-1}. We showed that the one-component inversion well predicts the observed NCP in the limb-side penumbra, but the agreement on the disk center-side is generally not as good as for the limb-

side. We conclude that the Evershed flows embedded in deep layer of the photosphere are associated with a stronger magnetic field than the upper layer. This findings is consistent with the result by Borrero and Solank (2008) for a sunspot observed on 2007 May 3, which shows a stronger magnetic field with an increased LOS velocity at the continuum level in the penumbra. In addition, our findings supports the recent numerical radiative MHD simulation by Rempel (2011), in which the convective hot gas penetrating up to the photosphere are associated with a strong radial magnetic field and the Lorentz force takes an important role for accelerating the horizontal Evershed flow (see Fig. 17 therein).

A dominant positive NCP structures in the disk center-side of the penumbra originates in the interflow channels rather than the Evershed flow. There are detectable flows in deep layer in the interflow channel too, in which there are a significant negative jump of field strength along the depth and a significant jump of the field inclination. These physical parameters make the positive NCP in the disk center-side penumbra. We recognized that a strong positive correlation between the LOS velocity and the magnetic field strength along the optical depth is a common feature in the Evershed flow channels. This topology has not been clearly recognized in previous observational works. Therefore we conclude that the Hinode observations of NCP in sunspot penumbra support the scenario, in which the flowing gas is strongly magnetized and the flow is accelerated or deflected to horizontal direction by the Lorentz force. Simple two component models of the penumbra, in which the Evershed flow embedded in alternate radial channels is responsible for the NCP, are not consistent with our result.

Acknowledgements

The authors are grateful to Dr. Bellot Rubio for valuable comments on SIR study, and Tetsu Anan and Dr. Hiroko Watanabe for their help in data analysis. The first author wants to express his great thanks to the Egyptian government for supporting his study in Japan. This work was partly supported by a Grant-in-Aid for Scientific Research (No. 22244013, PI: K. Ichimoto) from the Ministry of Education, Culture, Sports, Science and Technology of Japan. Hinode is a Japanese mission developed and launched by ISAS/JAXA, with NAOJ as domestic partner and NASA and STFC (UK) as international partners. It is operated by these agencies in cooperation with ESA and NSC (Norway).

References

Auer, L. H., Heasley, J. N. 1978, A&A, 64, 67

Beck, C. 2011, A&A 525, A133

Bellot Rubio, L. R., Balthasar, H., Collados, M. 2004, A&A, 427, 319

Bellot Rubio, L. R., Schlichenmaier, R., Tritschler, A. 2006, A&A, 453, 1117

Borrero, J. M., Solanki, S. K., Bellot Rubio, L. R., Lagg, A., Mathew, S. K. 2004, A&A, 422, 1093

Borrero, J. M., Solanki, S. K., Lagg, A., Socas-Navarro, H., Lites, B. 2006, A&A, 450, 383

Borrero, J. M.; Solanki, S. K. 2008, ApJ, 687, 668

Borrero, J. M., Lites, B. W., Solanki, S. K. 2008, A&A, 481, 13

Borrero, J.M., Ichimoto, K. 2011, LRSP, 8, 4

del Toro Iniesta, J. C., Tarbell, T. D., & Ruiz Cobo, B. 1994, ApJ, 436, 400

Henson, G. D., Kemp, J. C. 1984, Sol. Phys., 93, 289

Ichimoto, K. 2010, in Magnetic Coupling between the Interior and Atmosphere of the Sun, (Ed.)

Ichimoto, K., Shine, R. A., Lites, B., et al. 2007a, PASJ, 59, 593

Ichimoto, K., Suematsu, Y., Tsuneta, S., et al. 2007b, Science, 318, 1597

Ichimoto, K., Tsuneta, S., Suematsu, Y., et al. 2008, A&A, 481, L9

Illing, R. M. E., et al. 1974, A&A, 35, 327

Jurcak, J., Bellot Rubio, L., Ichimoto, K., et al. 2007, PASJ, 59, 601

Kosugi, T., et al. 2007, Sol. Phys., 243, 3

Langhans, K., Scharmer, G. B., Kiselman, et al. 2005, A&A, 436, 1087

Lites, B. W., Ichimoto, K. 2013, SoPh, 283, 601L

Martinez Pillet, V. 2000, A&A, 361, 734

Müller, D. A. N., Schlichenmaier, R., Steiner, O., Stix, M. 2002, A&A, 393, 305

Müller, D. A. N., Schlichenmaier, R., Fritz, G., Beck, C. 2006, A&A, 460

Press, W. H., Flannery, B. P., Teukolsky, S. A., Vetterling, W. T. 1986, Numerical Recipes (Cambridge Univ. Press)

Rempel, M., et al. 2009, Science, 325, 17

Rempel, M., 2011, arXiv: 1101.2200v1 [astro-ph.SR]

Rimmele, T., Marino, J. 2006, ApJ, 646, 593

Ruiz Cobo, B., del Toro Iniesta, J. C. 1992, ApJ, 398, 375

Sanchez Almeida, J., Lites, B. W. 1992, ApJ, 398, 359

Scharmer, G., Spruit, H. 2006, A&A, 460, 605

Scharmer, G. B., Nordlund, A, Heinemann, T. 2008, ApJ, 677, 149

Shine, R. A., Title, A. M., Tarbell, T. D., et al. 1994, ApJ, 430, 413

Skumanich, A., Lites, B. W. 1987, ApJ, 322, 483

Solanki, S. K. 2003, A&AR, 11, 153

Solanki, S. K., Montavon, C. A. P. 1993, A&A, 275, 283

Spruit, H., Scharmer, G. 2006, A&A, 447, 343

Spruit, H. C., Scharmer, G. B., Lofdahl, M. G., 2010, A&A, 521, 72

Suematsu, Y., Tsuneta, S., Ichimoto, K., et al. 2007, Sol. Phys., 249, 197S

Title, A. M., Frank, Z. A., Shine, R. A., et al. 1992, sto..work 195T

Tritschler, A., Schlichenmaier, R., Bellot Rubio, L. R., et al. 2004, A&A, 415, 717

Tritschler, A., Müller, D. A. N., Schlichenmaier, R., Hagenaar, H. J. 2007, ApJ, 671, L85

Tsuneta, S., et al. 2007, Sol. Phys., 249, 167

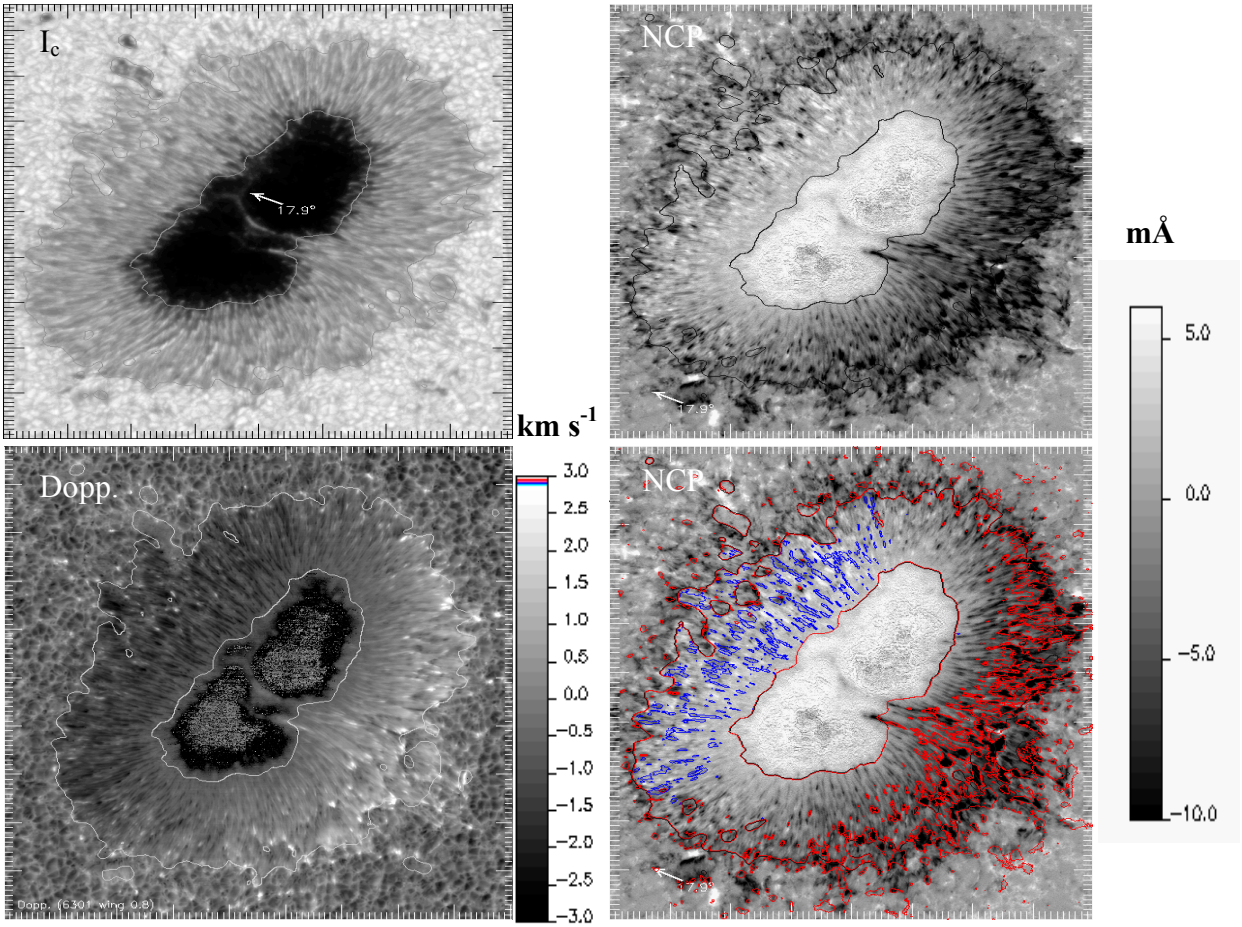

Fig. 1. The images include the sunspot observed on 15 Nov. 2006. Top row, left to right: continuum intensity and NCP. Bottom row, left to right: LOS velocity and NCP overlaid with contours of LOS velocity. The NCP and LOS velocity are scaled over the range of -10 ~ +6 mÅ and -3 ~ +3 km s^{-1}, respectively. As is evident in the Dopplergram, red shift is white and blue shift is black. LOS velocities are displayed by red and blue contours in NCP map with -1.5 (blue) and 0.8 (red) km s^{-1}. The arrow in the continuum map shows the direction to disk center. Interval of minor ticks is 1 arcsec.

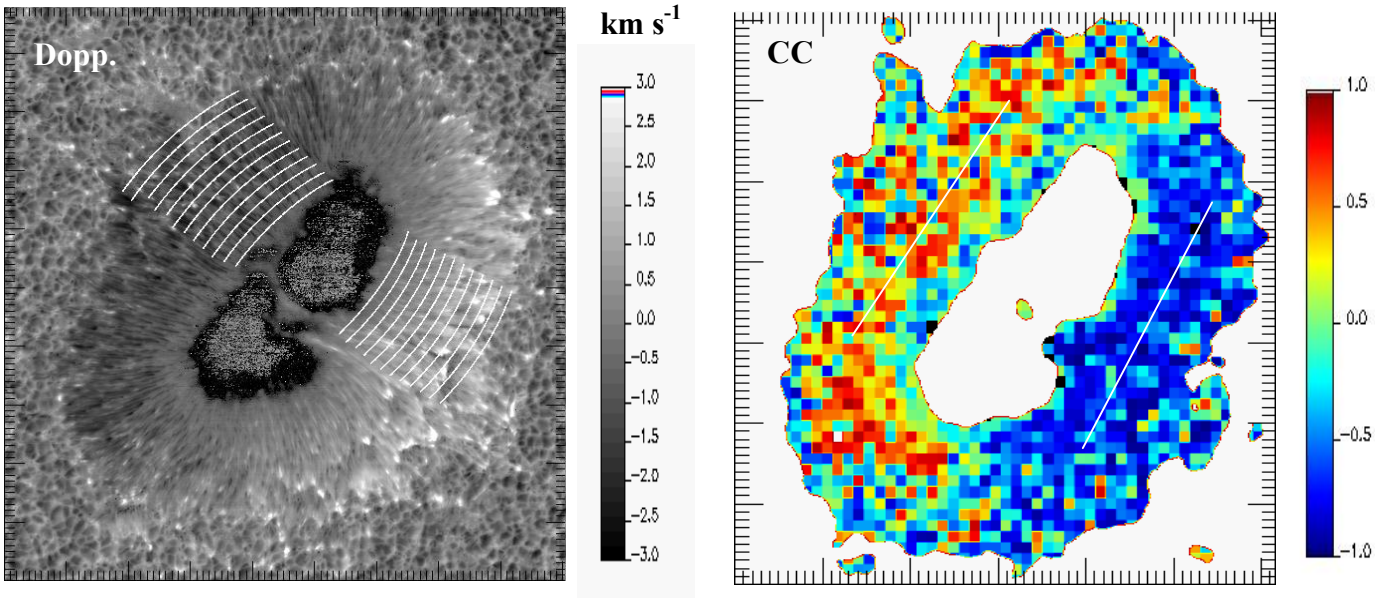

Fig. 2. Left to right: LOS velocity and correlation coefficients (CC) between NCP and LOS velocity. The CC map is scaled over the range of -1 ~ 1. The region used for azimuthally averages in the photosphere is displayed by thin arcs in the Doppler map (left panel). As shown in the CC map (right panel), the two azimuthal cuts represent the locations selected for the fitting at the middle limb-side and disk center-side penumbra.

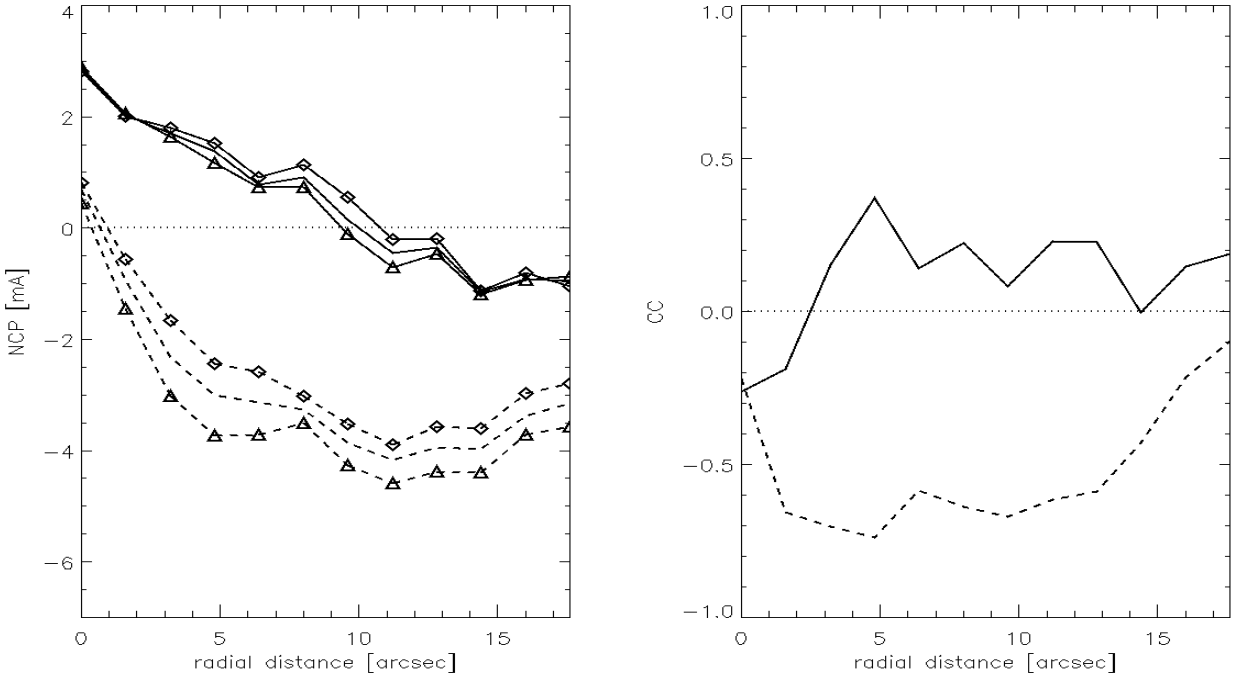

Fig. 3. Azimuthally averaged NCP (left) and correlation coefficient (CC) between LOS velocity and NCP (right) as a function of the radial distance from the inner edge of penumbra. Curves represented by dashed lines correspond to the azimuthally averages in the limb-side and the curves indicated by solid lines to the averages in the disk center-side of the penumbra, while curves marked with triangles and diamonds refer to the Evershed flow and the interflow channels, respectively. Note that a radial distance of zero arcsec exhibits the inner edge of penumbra, and a radial distance of 18 arcsec displays the outer edge.

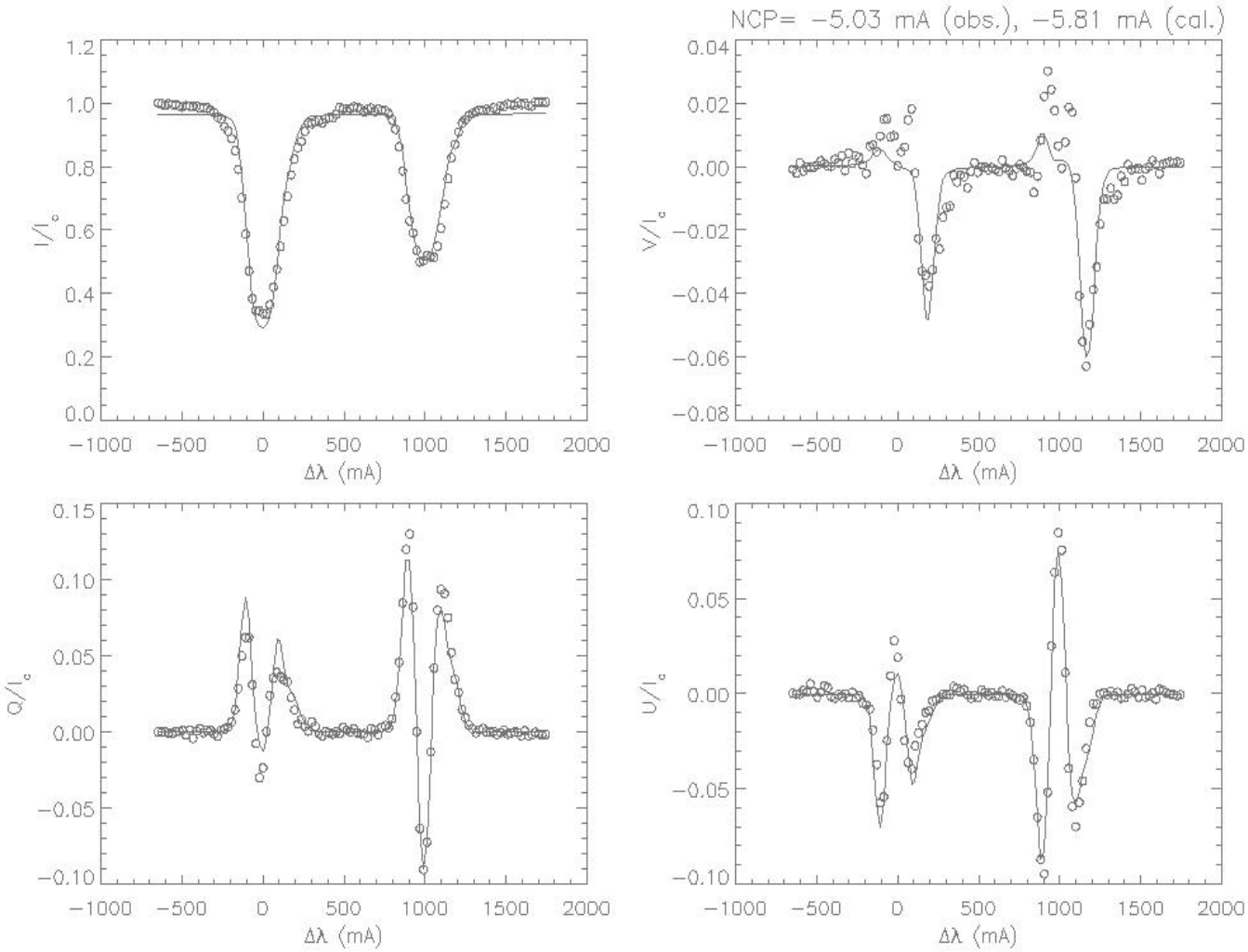

Fig. 4. The observed Stokes I, Q, U and V profiles (circles) and the synthetic profiles (solid lines). This example shows the fitting of the Stokes profiles in the Evershed flow channels in limb-side of the penumbra.

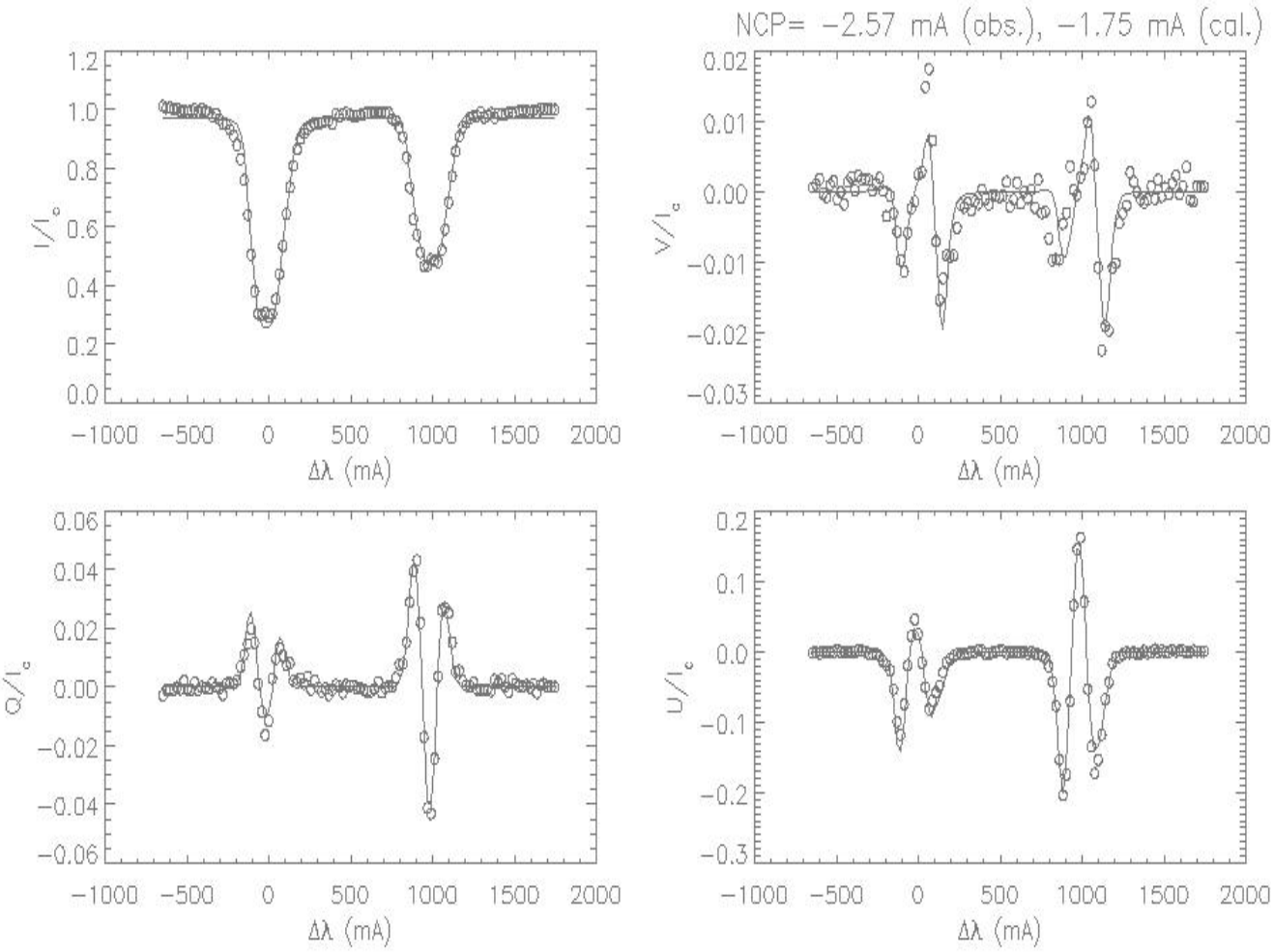

Fig. 5. Same as Fig. 4, but for the interflow channel in limb-side penumbra.

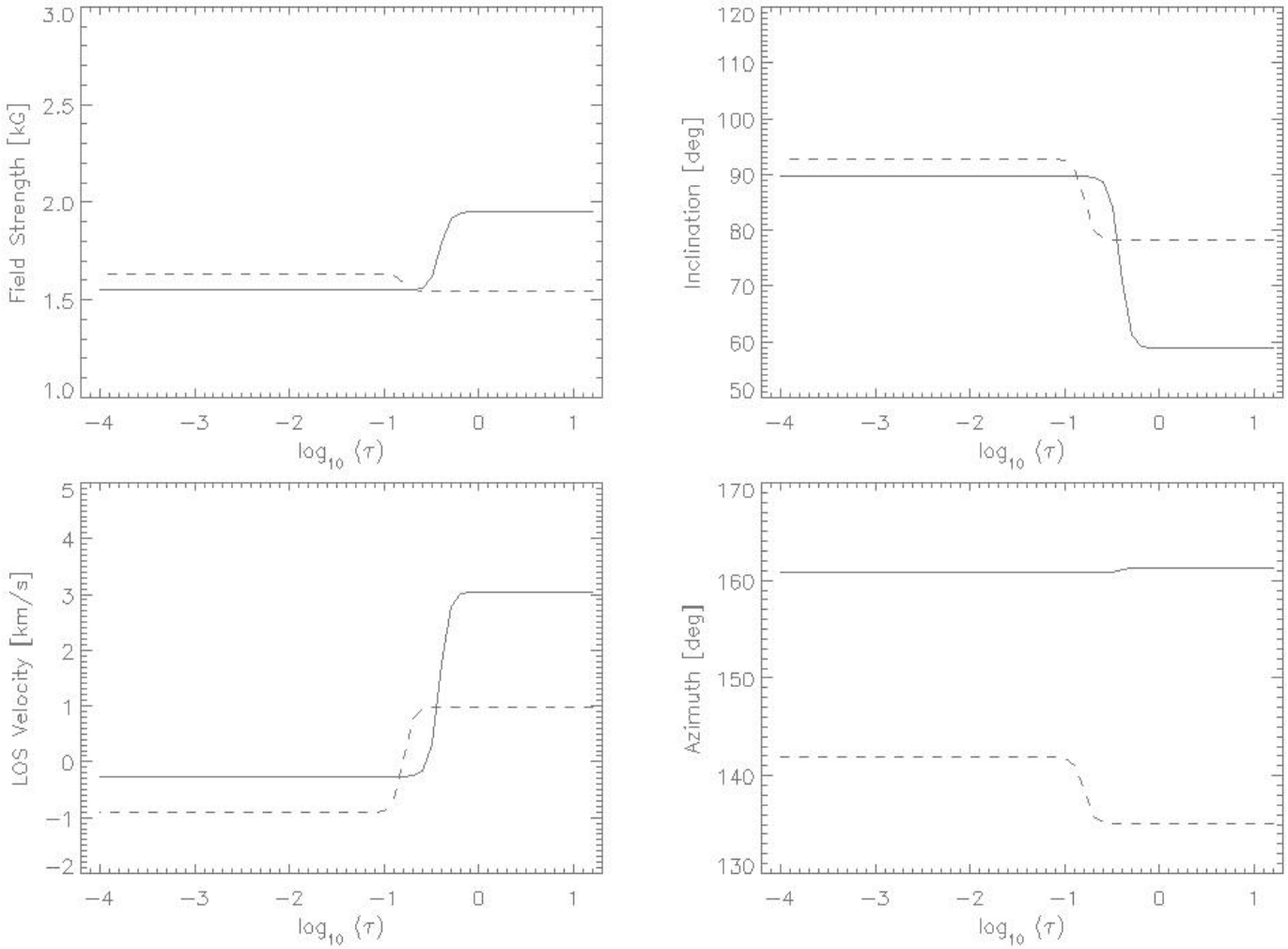

Fig. 6. The stratifications of the magnetic field strength, inclination, LOS velocity and azimuth obtained using the SIR-JUMP inversion code. Curves represented by solid lines and dashed lines show the Evershed and interflow channels in limb-side penumbra, respectively.

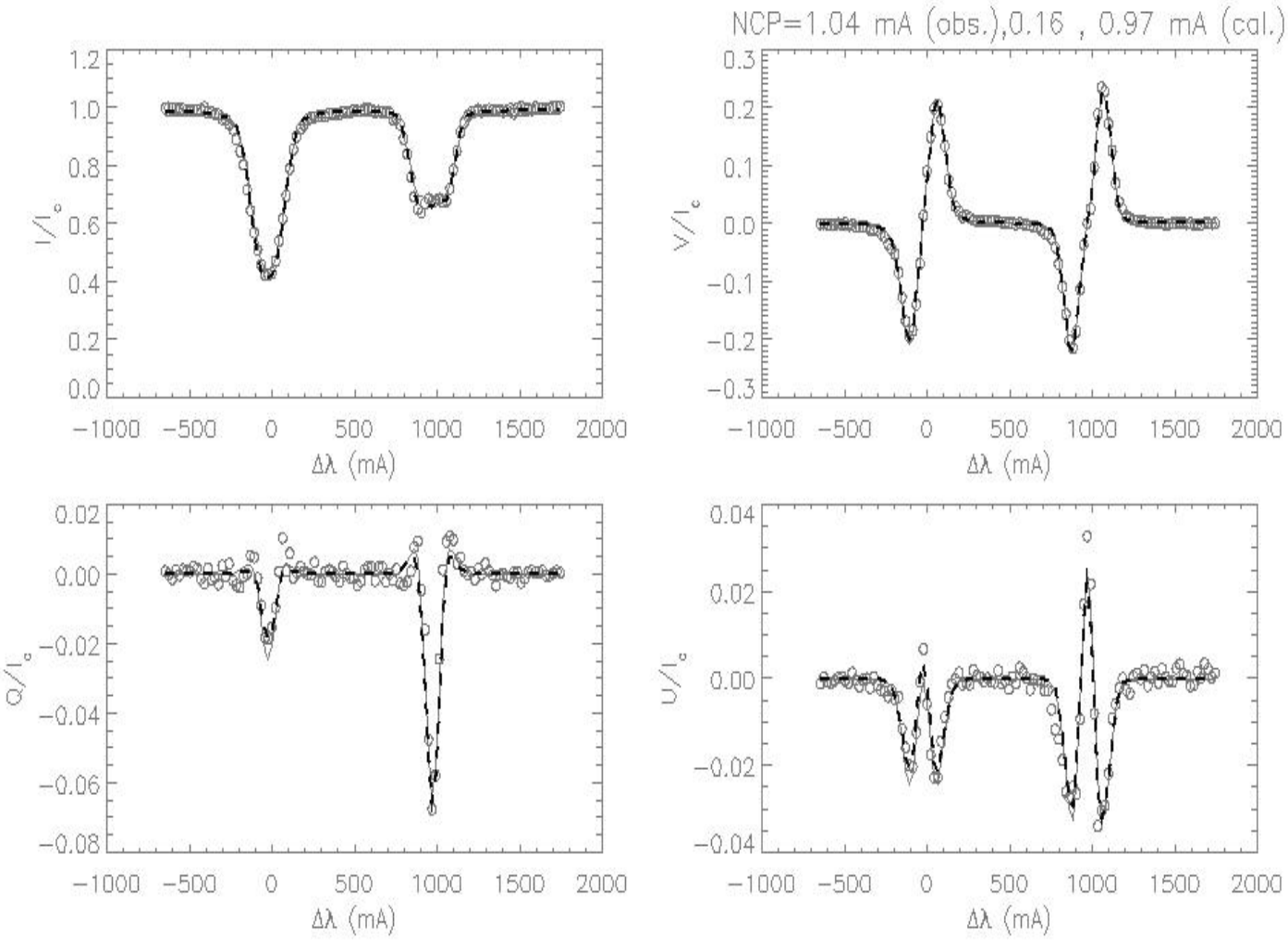

Fig. 7. The same as Fig. 4 but for the Evershed flow channel in the disk center-side penumbra. This figure represents the synthetic Stokes profiles (solid and thick dashed lines) from the two solutions displayed by solid and dashed lines in Fig. 8 for the selected pixel showing the ambiguity (= non uniqueness of solution) of inversion.

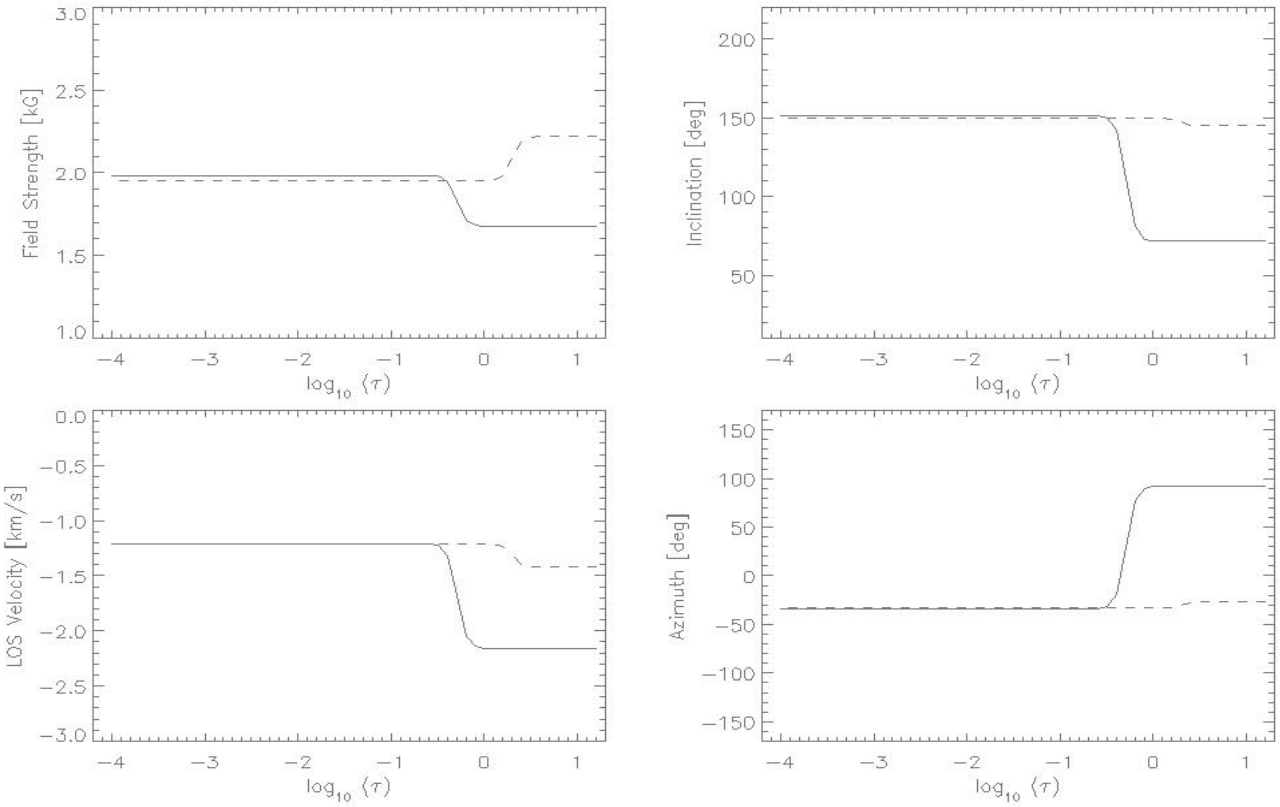

Fig. 8. The same as Fig. 6 but for Evershed flow channels in the disk center-side of the penumbra. Here we show two solutions of the physical stratifications for the selected pixel obtained with the fitting results displayed in Fig. 7.

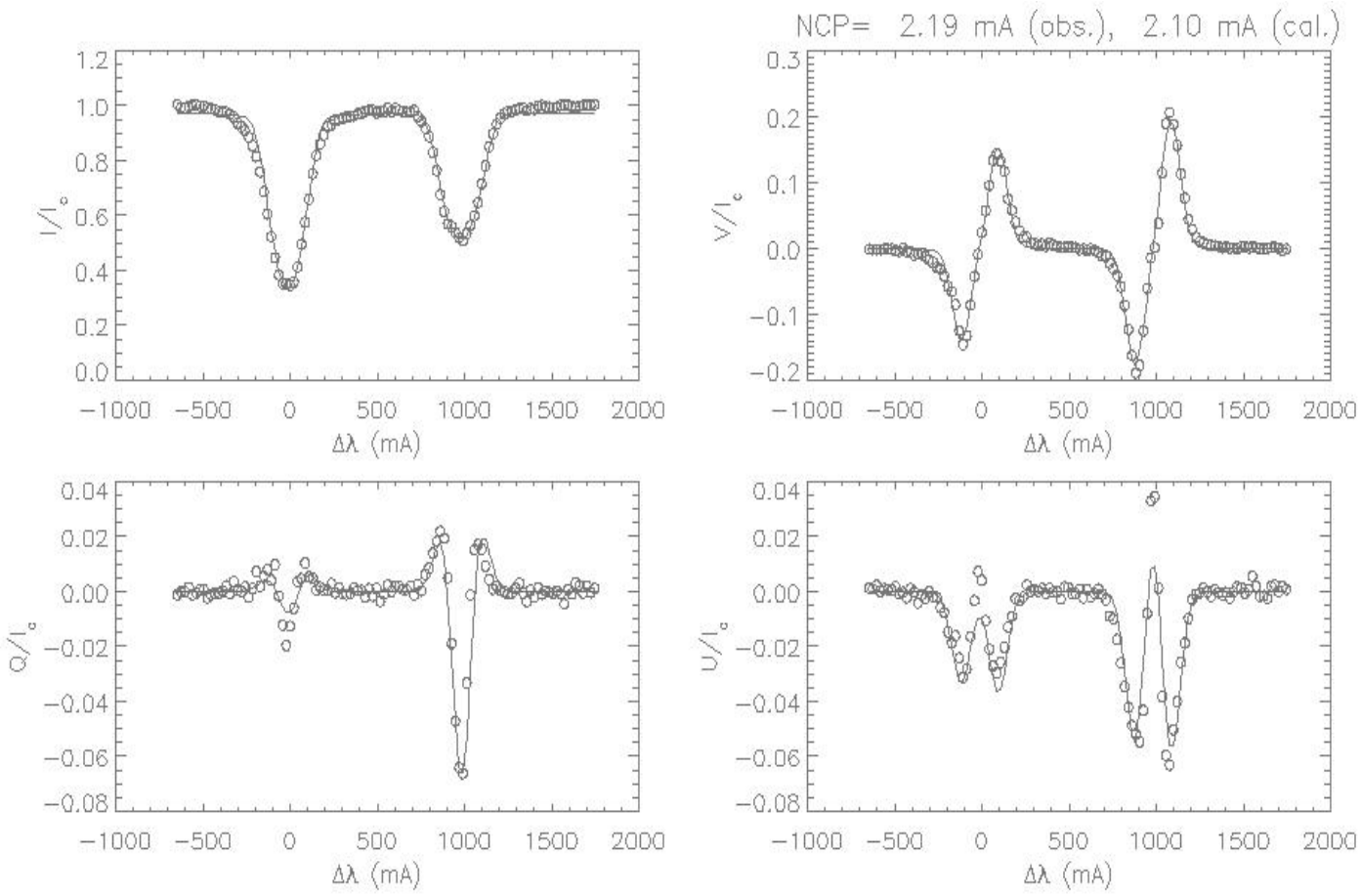

Fig. 9. Same as Fig. 5, but for the interflow channel in disk center-side penumbra.

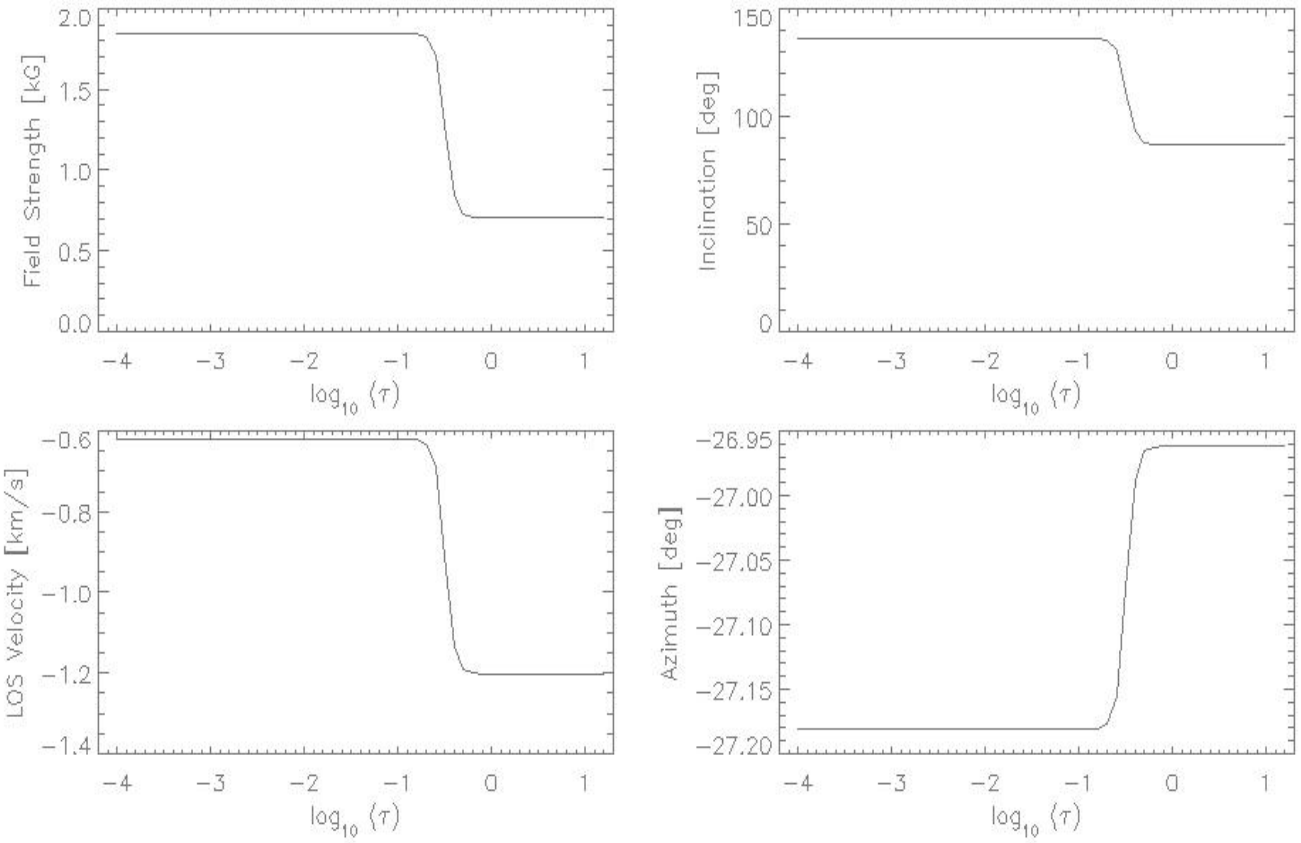

Fig. 10. Same as Fig. 6, but for the interflow channel in disk center-side penumbra.

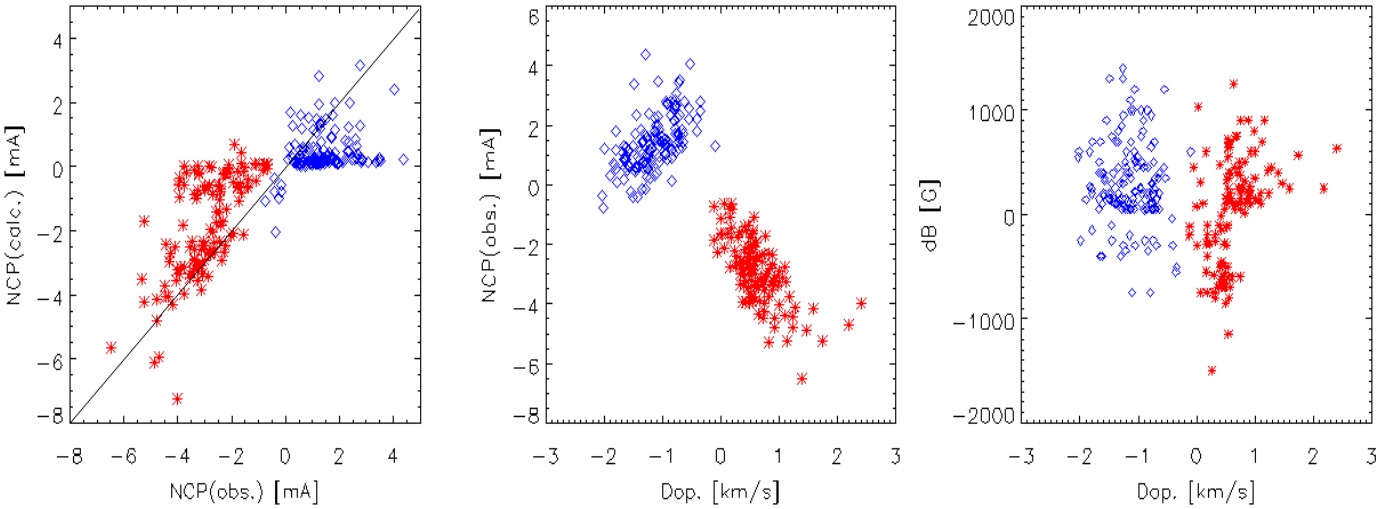

Fig. 11. The NCP of the best-fit Stokes V profiles against the observed NCP (left), observed NCP versus LOS velocity (middle) and amplitude of the discontinuity of the field strength (dB) versus LOS velocity (right). Red asterisks show the values in the limb-side, while blue diamonds represent the values for the disk center-side penumbra.